

On the Closed-form Proximal Mapping and Efficient Algorithms for Exclusive Lasso Models

Yancheng Yuan[†] Meixia Lin[‡] Defeng Sun[§] Kim-Chuan Toh[¶]

January 28, 2019

Abstract

The exclusive lasso regularization based on the $\ell_{1,2}$ norm has become popular recently due to its superior performance over the group lasso regularization. Comparing to the group lasso regularization which enforces the competition on variables among different groups and results in inter-group sparsity, the exclusive lasso regularization also enforces the competition within each group and results in intra-group sparsity. However, to the best of our knowledge, a correct closed-form solution to the proximal mapping of the $\ell_{1,2}$ norm has still been elusive. In this paper, we fill the gap by deriving a closed-form solution for $\text{Prox}_{\rho\|\cdot\|_2^2}(\cdot)$ and its generalized Jacobian. Based on the obtained analytical results, we are able to design efficient first and second order algorithms for machine learning models involving the exclusive lasso regularization. Our analytical solution of the proximal mapping for the exclusive lasso regularization can be used to improve the efficiency of existing algorithms relying on the efficient computation of the proximal mapping.

Keywords: Exclusive lasso, semismooth Newton method, augmented Lagrangian method, proximal mapping

1 Introduction

Structured sparsity is very important in representation learning, not only for avoiding over-fitting, but also in making the model more interpretable. Many regularizers and their combinations have been proposed to enforce sparsity for parameterized machine learning models [25, 26, 32, 31]. The most popular among them are probably

[†]Department of Mathematics, National University of Singapore, 10 Lower Kent Ridge Road, Singapore (yuanyancheng@u.nus.edu).

[‡]Department of Mathematics, National University of Singapore, 10 Lower Kent Ridge Road, Singapore (lin_meixia@u.nus.edu).

[§]Department of Applied Mathematics, The Hong Kong Polytechnic University, Hung Hom, Hong Kong (defeng.sun@polyu.edu.hk).

[¶]Department of Mathematics and Institute of Operations Research and Analytics, National University of Singapore, 10 Lower Kent Ridge Road, Singapore (matttohkc@nus.edu.sg).

the standard lasso [25] and group lasso [32, 31] regularizers. Lasso, group lasso and their variants have been intensively studied in terms of both their statistical properties [25, 5, 36, 39, 32, 4] and efficient numerical computations [7, 18, 2, 28, 31, 13, 35]. The lasso model has been important in enforcing sparsity and feature selections, however, there is no structure enforced in the sparsity pattern. Instead, the group lasso is known to enforce the sparsity at an inter-group level where variables from different groups compete to be selected. The idea behind the group lasso is that if a few features in one feature group are important, then most of the features in the same group should also be important. Thus, in the group lasso, the whole winning groups will obtain large coefficients, but zeros for losing groups.

However, in some real applications, instead of the unstructured sparsity (e.g. lasso) or inter-group level structured sparsity (e.g. group lasso), we also need an intra-group level sparsity. That is, not only features from different groups, but also features in a seemingly cohesive group are competing to survive. One real example is building an index exchange-traded fund (index ETF) to track some particular indices in the stock markets. To diversify the risks across different sectors, we need to do portfolio selection both across and within sectors together, which indeed means that we also need an intra-group level sparsity. To achieve this, a new regularizer called the exclusive lasso has been proposed in [38, 11]. For any $\mathbf{x} \in \mathbb{R}^n$ and a partition of index sets $\mathcal{G} := \{g | g \subseteq \{1, 2, \dots, n\}\}$ such that $\bigcup_{g \in \mathcal{G}} g = \{1, 2, \dots, n\}$ and $g_1 \cap g_2 = \emptyset$ for $\forall g_1, g_2 \in \mathcal{G}$, the exclusive lasso regularizer is defined as

$$\Omega_{EL}^{\mathcal{G}}(\mathbf{x}) := \sum_{g \in \mathcal{G}} \|\mathbf{x}_g\|_1^2. \quad (1)$$

For the exclusive lasso regularizer, an ℓ_2 norm is applied to the ℓ_1 norm of different groups, and within each group, an ℓ_1 norm is used to enforce sparsity. Thus, the exclusive lasso regularizer is also known as the $\ell_{1,2}$ norm.

The exclusive lasso regularizer was first proposed for multi-task learning [38] and has been widely applied in applications for obtaining an intra-group level structured sparsity [11, 3, 34, 30, 29, 27]. Some efficient numerical optimization algorithms have been proposed for solving machine learning models involving the exclusive lasso regularization. Because there is no closed-form solution available previously for $\text{Prox}_{\rho \|\cdot\|_1^2}(\cdot)$, it was perceived to be inefficient to directly apply some popular algorithmic frameworks like the accelerated proximal gradient (APG) [18], FISTA [2] and alternating direction method of multipliers (ADMM) [9, 6]. Kong et al. [11] designed an iterative least squares algorithm which is now popular in solving machine learning models involving the exclusive lasso regularization. Campbell et. al [3] adopted a proximal gradient method to solve the exclusive lasso model with an iterative subroutine to compute $\text{Prox}_{\rho \|\cdot\|_1^2}(\cdot)$. Recently, Yoon et. al [30] proposed to combine the group lasso and the exclusive lasso regularizations together and applied them in a deep neural network to obtain structured sparsity. In their paper, the authors used the stochastic proximal gradient algorithm to solve the corresponding optimization problem that is highly dependent on the efficient computation of the proximal mapping of the exclusive lasso regularizer. They also proposed a closed-form solution to $\text{Prox}_{\rho \|\cdot\|_1^2}(\cdot)$. However, unfortunately, the proposed solution is incorrect as we shall discuss in the next section [see Remark 1].

In this paper, we first derive the closed-form solution to the proximal mapping of the exclusive lasso regularizer. As mentioned above, such a closed-form solution will improve the computational efficiency of algorithms such as the APG and ADMM for solving machine learning models involving the exclusive lasso regularizer. Furthermore, we also derive the generalized Jacobian of $\text{Prox}_{\rho\|\cdot\|_1^2}(\cdot)$. Based on these analytical results, we will design a second-order type algorithm, known as the semismooth Newton-CG based augmented Lagrangian method (SSNAL), to solve the exclusive lasso model. We summarize our main contributions in this paper as follows. (1) We derive the closed-form solution of the proximal mapping of $\|\cdot\|_1^2$ and the corresponding generalized Jacobian. These results are critical for the computational efficiency of various algorithmic frameworks. (2) We propose a semismooth Newton-CG based augmented Lagrangian method to solve the exclusive lasso model. (3) We demonstrate numerically that SSNAL is highly efficient and robust comparing to popular first-order algorithms such as APG and ADMM, even with employing the closed-form proximal mapping of the exclusive lasso regularizer we derived in this paper. Furthermore, we apply the exclusive lasso model in partial financial index tracking and achieve better out-of-sample results, comparing to lasso.

The remaining parts of the paper are organized as follows. We derive the closed-form solution to $\text{Prox}_{\rho\|\cdot\|_1^2}(\cdot)$ and its generalized Jacobian in section 2. The SSNAL algorithm for solving the general two block convex composite programming and the corresponding semismooth Newton-CG method (SSNCG) for solving the subproblem will be introduced in section 3. In section 4, we present our numerical results on both synthetic data and real applications in finance. In the end, we conclude the paper and discuss some possible feature work.

2 Closed-form solution to the proximal mapping of $\|\cdot\|_1^2$ and its generalized Jacobian

In this section, we derive the closed-form solution of $\text{Prox}_{\rho\|\cdot\|_1^2}(\cdot)$ and its generalized Jacobian. These results are crucial for us to design an efficient algorithm to solve the exclusive lasso regularized machine learning models in the next section.

2.1 Closed-form solution to $\text{Prox}_{\rho\|\cdot\|_1^2}(\cdot)$

For a given $\mathbf{a} \in \mathbb{R}^n$ and $\rho > 0$, the proximal mapping $\text{Prox}_{\rho\|\cdot\|_1^2}(\cdot)$ at point \mathbf{a} is the solution to the following optimization problem:

$$\min_{\mathbf{x} \in \mathbb{R}^n} \frac{1}{2} \|\mathbf{x} - \mathbf{a}\|^2 + \rho \|\mathbf{x}\|_1^2. \quad (2)$$

Note that the objective function of (2) is invariant under the permutation of the indices. We first derive the closed-form solution of $\text{Prox}_{\rho\|\cdot\|_1^2}(\mathbf{a})$ for the special case where $\mathbf{a}_1 \geq \mathbf{a}_2 \geq \dots \geq \mathbf{a}_n \geq 0$.

Proposition 1 For given $\rho > 0$ and a nonzero vector $\mathbf{a} \in \mathbb{R}^n$ such that $\mathbf{a}_1 \geq \mathbf{a}_2 \geq \dots \geq \mathbf{a}_n \geq 0$. We have

(a) The optimal solution \mathbf{x}^* to (2) has the property that

$$\mathbf{x}_1^* \geq \mathbf{x}_2^* \geq \dots \geq \mathbf{x}_n^* \geq 0.$$

(b) Denote

$$s_i = \sum_{j=1}^i \mathbf{a}_j, \quad \alpha_i = \frac{2\rho s_i}{1 + 2i\rho}, \quad i = 1, 2, \dots, n.$$

Let k be the largest index such that $\alpha_k = \max_{1 \leq i \leq n} \alpha_i$. Then, the optimal solution to (2) is given as follows:

$$\mathbf{x}_i^* = \begin{cases} \mathbf{a}_i - \alpha_k, & \text{if } i = 1, \dots, k, \\ 0, & \text{if } i = k + 1, \dots, n. \end{cases}$$

Proof 1 (a) Suppose there exists $i < j$ but $\mathbf{x}_i^* < \mathbf{x}_j^*$. Consider $\hat{\mathbf{x}}$ such that $\hat{\mathbf{x}}_k = \mathbf{x}_k^*$ for $k \neq i, j$ and $\hat{\mathbf{x}}_i = \mathbf{x}_j^*$, $\hat{\mathbf{x}}_j = \mathbf{x}_i^*$. Then

$$\begin{aligned} & \frac{1}{2}(\|\mathbf{x}^* - \mathbf{a}\|^2 - \|\hat{\mathbf{x}} - \mathbf{a}\|^2) + \rho(\|\mathbf{x}^*\|_1^2 - \|\hat{\mathbf{x}}\|_1^2) \\ &= \frac{1}{2}(\|\mathbf{x}^* - \mathbf{a}\|^2 - \|\hat{\mathbf{x}} - \mathbf{a}\|^2) \\ &= (\mathbf{a}_j - \mathbf{a}_i)(\mathbf{x}_i^* - \mathbf{x}_j^*) \geq 0. \end{aligned}$$

Thus, $\hat{\mathbf{x}}$ is also a minimizer to (2). Since the objective function in (2) is strongly convex, the optimal solution is unique. However, $\mathbf{x}^* \neq \hat{\mathbf{x}}$, which is a contradiction. Thus we must have $\mathbf{x}_1^* \geq \mathbf{x}_2^* \geq \dots \geq \mathbf{x}_n^*$.

Next we show that $\mathbf{x}_n^* \geq 0$. Suppose on the contrary that $\mathbf{x}_n^* < 0$. Then we can construct $\bar{\mathbf{x}}$ such that $\bar{\mathbf{x}}_k = \mathbf{x}_k^*$ for $k \neq n$, and $\bar{\mathbf{x}}_n = -\mathbf{x}_n^* > 0$. Now

$$\begin{aligned} & \frac{1}{2}(\|\mathbf{x}^* - \mathbf{a}\|^2 - \|\bar{\mathbf{x}} - \mathbf{a}\|^2) + \rho(\|\mathbf{x}^*\|_1^2 - \|\bar{\mathbf{x}}\|_1^2) \\ &= -2\mathbf{a}_n \mathbf{x}_n^* \geq 0. \end{aligned}$$

Thus $\bar{\mathbf{x}}$ is also a minimizer. By the uniqueness of \mathbf{x}^* , we get a contradiction again. Thus we must have $\mathbf{x}_n^* \geq 0$.

(b) With the result in (a), the solution to (2) could be found by solving

$$\begin{aligned} & \min_{\mathbf{x}} \left\{ \frac{1}{2} \|\mathbf{x} - \mathbf{a}\|^2 + \rho \left(\sum_{i=1}^n \mathbf{x}_i \right)^2 \mid \mathbf{x}_1 \geq \dots \geq \mathbf{x}_n \geq 0 \right\} \\ &= \min_{\mathbf{x}} \left\{ \frac{1}{2} \|\mathbf{x} - \mathbf{a}\|^2 + \rho \mathbf{x}^T (\mathbf{e}\mathbf{e}^T) \mathbf{x} \mid C\mathbf{x} \geq 0 \right\}, \end{aligned} \quad (3)$$

where $C \in \mathbb{R}^{n \times n}$ is the forward-difference matrix with its last row appended by \mathbf{e}_n^T , and $\mathbf{e} \in \mathbb{R}^n$ is the vector of all ones. The Karush-Kuhn-Tucker (KKT) conditions for (3) are given by

$$\begin{aligned} & \mathbf{x}^* - \mathbf{a} + 2\rho\mathbf{e}\mathbf{e}^T \mathbf{x}^* - C^T \boldsymbol{\mu}^* = 0, \\ & \boldsymbol{\mu}^* \circ C\mathbf{x}^* = 0, \quad \boldsymbol{\mu}^* \geq 0, \quad C\mathbf{x}^* \geq 0, \end{aligned} \quad (4)$$

where $\boldsymbol{\mu}^* \in \mathbb{R}^n$ is the dual multiplier and “ \circ ” denotes the Hadamard product. We consider the following cases.

(i) $2 \leq k \leq n - 1$. By the definition of k , we have

$$\begin{aligned}
0 &\leq \alpha_k - \alpha_{k-1} \\
&= \frac{2\rho s_k}{1+2k\rho} - \frac{2\rho s_{k-1}}{1+2(k-1)\rho} \\
&= \frac{(1+2(k-1)\rho)2\rho s_k - (1+2k\rho)2\rho s_{k-1}}{(1+2k\rho)(1+2(k-1)\rho)} \\
&= \frac{2\rho[(1+2k\rho)\mathbf{a}_k - 2\rho s_k]}{(1+2k\rho)(1+2(k-1)\rho)} \\
&= \frac{2\rho(1+2k\rho)(\mathbf{a}_k - \alpha_k)}{(1+2k\rho)(1+2(k-1)\rho)}.
\end{aligned}$$

Thus, $\mathbf{a}_k \geq \alpha_k$. Furthermore,

$$\begin{aligned}
0 &< \alpha_k - \alpha_{k+1} \\
&= \frac{2\rho s_k}{1+2k\rho} - \frac{2\rho s_{k+1}}{1+2(k+1)\rho} \\
&= \frac{(1+2(k+1)\rho)2\rho s_k - (1+2k\rho)2\rho s_{k+1}}{(1+2k\rho)(1+2(k+1)\rho)} \\
&= \frac{2\rho(1+2k\rho)(\alpha_k - \mathbf{a}_{k+1})}{(1+2k\rho)(1+2(k+1)\rho)},
\end{aligned}$$

which implies that $\alpha_k > \mathbf{a}_{k+1}$. As a result, $\mathbf{a}_1 \geq \dots \geq \mathbf{a}_k \geq \alpha_k > \mathbf{a}_{k+1} \geq \dots \geq \mathbf{a}_n \geq 0$. Consider

$$\mathbf{x}_i^* = \begin{cases} \mathbf{a}_i - \alpha_k, & \text{if } i = 1, \dots, k, \\ 0 & \text{if } i = k+1, \dots, n; \end{cases}$$

$$\boldsymbol{\mu}_i^* = \begin{cases} 0, & \text{if } i = 1, \dots, k, \\ \sum_{j=k+1}^i (\alpha_k - \mathbf{a}_j) & \text{if } i = k+1, \dots, n. \end{cases}$$

It is not difficult to check that $(\mathbf{x}^*, \boldsymbol{\mu}^*)$ satisfies the KKT conditions (4). Hence, \mathbf{x}^* is the optimal solution to (3).

(ii) $k = n$. Then $\alpha_{n-1} \leq \alpha_n$ implies that $\mathbf{a}_n - \alpha_n \geq 0$. Hence $\mathbf{a}_i \geq \alpha_n, \forall i = 1, 2, \dots, n$. It is easy to verify that

$$\mathbf{x}^* = \mathbf{a} - \alpha_n \mathbf{e}, \quad \boldsymbol{\mu}^* = 0,$$

is a solution to the KKT conditions (4).

(iii) $k = 1$. Then $\alpha_1 - \alpha_2 > 0$ implies that $\alpha_1 - \mathbf{a}_2 > 0$. Also, we can see that

$$\alpha_1 = \frac{2\rho}{1+2\rho} \mathbf{a}_1 \leq \mathbf{a}_1.$$

Consider

$$\mathbf{x}_i^* = \begin{cases} \mathbf{a}_i - \alpha_1 & \text{if } i = 1, \\ 0 & \text{if } i = 2, \dots, n, \end{cases}$$

$$\boldsymbol{\mu}^* = \begin{cases} 0 & \text{if } i = 1, \\ \sum_{j=2}^i (\alpha_1 - \mathbf{a}_j) & \text{if } i = 2, \dots, n. \end{cases}$$

Now we can verify that the above pair $(\mathbf{x}^*, \boldsymbol{\mu}^*)$ is a solution to the KKT conditions (4).

With the results above, we now give the closed-form solution to $\text{Prox}_{\rho\|\cdot\|_1^2}(\mathbf{a})$ for any $\mathbf{a} \in \mathbb{R}^n$.

Proposition 2 For given $\rho > 0$ and a nonzero vector $\mathbf{a} \in \mathbb{R}^n$. Let $\Pi \in \mathbb{R}^{n \times n}$ be the permutation matrix such that $\Pi|\mathbf{a}| = \mathbf{b}$ where $\mathbf{b}_1 \geq \mathbf{b}_2 \geq \dots \geq \mathbf{b}_n \geq 0$. Then we have

$$\text{Prox}_{\rho\|\cdot\|_1^2}(\mathbf{a}) = \text{sign}(\mathbf{a}) \circ \Pi^T(\text{Prox}_{\rho\|\cdot\|_1^2}(\mathbf{b})),$$

where $\text{Prox}_{\rho\|\cdot\|_1^2}(\mathbf{b})$ can be computed by Proposition 1. Consequently, $\text{Prox}_{\rho\|\cdot\|_1^2}(\mathbf{a})$ can be computed in $O(n \log n)$ operations.

Proof 2 Since the objective function in (2) is invariant to the permutation of the indices and $\|\mathbf{x}\|_1^2$ is invariant to the changes of signs, the conclusions of this proposition hold.

Remark 1 Here, we discuss briefly the incorrect closed-form solution to $\text{Prox}_{\rho\|\cdot\|_1^2}(\cdot)$ given in [30]¹:

$$\phi_\rho(\mathbf{a}) = \text{sign}(\mathbf{a}) \circ (|\mathbf{a}| - \rho\|\mathbf{a}\|_1)_+ \quad \forall \mathbf{a} \in \mathbb{R}^n.$$

Suppose that $\rho \geq 1$. Since $|\mathbf{a}_i| \leq \rho\|\mathbf{a}\|_1$ for any i , the above formula gives $\phi_\rho(\mathbf{a}) = \mathbf{0}$ for any given $\mathbf{a} \in \mathbb{R}^n$. However, it is readily shown that $\text{Prox}_{\rho\|\cdot\|_1^2}(\mathbf{a}) \neq \mathbf{0}$ if $\mathbf{a} \neq \mathbf{0}$. For example, when $n = 2$, $\mathbf{a} = (1, 1)^T$, one has $\text{Prox}_{\rho\|\cdot\|_1^2}(\mathbf{a}) = (1/9, 1/9)^T$ for $\rho = 2$. Actually, for $n = 1$, one can easily obtain that $\text{Prox}_{\rho\|\cdot\|_1^2}(\mathbf{a}) = \mathbf{a}/(1 + 2\rho)$ for any $\rho > 0$. Thus the closed-form solution given in [30] is incorrect.

2.2 The generalized Jacobian of $\text{Prox}_{\rho\|\cdot\|_1^2}(\cdot)$

Recently, the semismooth Newton-CG based augmented Lagrangian method (ALM) has been proven to be a powerful algorithmic framework for solving various convex conic optimization problems and convex machine learning models (e.g., [14, 33, 35, 13, 15]). The high efficiency of the framework mainly comes from the fast linear convergence of the ALM in the outer loop and the superlinear (even quadratic) convergence of the semismooth Newton method for solving the inner subproblems. In order to design a semismooth Newton-CG based ALM to solve models involving $\|\cdot\|_1^2$, it is critical for us to derive an explicit formula for some form of the generalized Jacobian of $\text{Prox}_{\rho\|\cdot\|_1^2}(\cdot)$. Here, we derive a specific element in the set of the so-called HS-Jacobian of $\text{Prox}_{\rho\|\cdot\|_1^2}(\cdot)$ based on the quadratic programming (QP) reformulation of the proximal problem of

¹We assume that in computing $\phi_\rho(\mathbf{a})$, the authors ignored the 1/2-factor in the definition of the exclusive sparsity regularization in (4) of [30], which is also incorrect even if this 1/2-factor is restored.

$\rho \|\cdot\|_1^2$. For a given $\mathbf{b} \in \mathbb{R}_+^n$ satisfying $\mathbf{b}_1 \geq \mathbf{b}_2 \geq \dots \geq \mathbf{b}_n \geq 0$, we know that $\text{Prox}_{\rho \|\cdot\|_1^2}(\mathbf{b})$ can be computed as

$$\mathbf{x}(\mathbf{b}) := \arg \min_{\mathbf{x} \in \mathbb{R}^n} \left\{ \frac{1}{2} \langle \mathbf{x}, Q\mathbf{x} \rangle - \langle \mathbf{x}, \mathbf{b} \rangle \mid C\mathbf{x} \geq 0 \right\}, \quad (5)$$

where $Q = I_n + 2\rho\mathbf{e}\mathbf{e}^T \in \mathbb{R}^{n \times n}$,

$$C\mathbf{x} = [\mathbf{x}_1 - \mathbf{x}_2; \dots, \mathbf{x}_{n-1} - \mathbf{x}_n; \mathbf{x}_n] \in \mathbb{R}^n. \quad (6)$$

Based on the above strongly convex QP, we can derive the HS-Jacobian of $\mathbf{x}(\mathbf{b})$ by applying the general results established in [10, 14], which we will describe in the ensuing paragraphs.

From the optimality of $\mathbf{x}(\mathbf{b})$, we know that there exist a multiplier $\boldsymbol{\lambda} \in \mathbb{R}^n$ such that

$$\begin{cases} Q\mathbf{x}(\mathbf{b}) - \mathbf{b} + C^T\boldsymbol{\lambda} = 0, \\ C\mathbf{x}(\mathbf{b}) \geq 0, \\ \boldsymbol{\lambda} \leq 0, \boldsymbol{\lambda}^T C\mathbf{x}(\mathbf{b}) = 0. \end{cases} \quad (7)$$

Let $M(\mathbf{b})$ be the set of corresponding multipliers, i.e.,

$$M(\mathbf{b}) := \{\boldsymbol{\lambda} \in \mathbb{R}^n \mid (\mathbf{x}(\mathbf{b}), \boldsymbol{\lambda}) \text{ satisfies (7)}\}.$$

Since $M(\mathbf{b})$ is a non-empty convex polyhedral set containing no lines, it has at least one extreme point [21, Corollary 18.5.3]. Denote the active set

$$I(\mathbf{b}) := \{i \in \{1, \dots, n\} \mid C_i\mathbf{x}(\mathbf{b}) = 0\}, \quad (8)$$

where C_i is the i th row of C . Now, we define a collection of index sets:

$$\begin{aligned} \mathcal{K}(\mathbf{b}) := & \{K \subseteq \{1, \dots, n\} \mid \exists \boldsymbol{\lambda} \in M(\mathbf{b}) \text{ s.t. } K \subseteq I(\mathbf{b}), \\ & \text{supp}(\boldsymbol{\lambda}) \subseteq K, C_K^T \text{ is of full column rank}\}, \end{aligned}$$

where $\text{supp}(\boldsymbol{\lambda})$ denotes the set of indices i such that $\lambda_i \neq 0$ and C_K is the matrix consisting of the rows of C , indexed by K . Due to the existence of the extreme point of $M(\mathbf{b})$, the set $\mathcal{K}(\mathbf{b})$ is non-empty [10]. Since the B-subdifferential $\partial_B\mathbf{x}(\mathbf{b})$ is usually very difficult to compute, in [14], generalizing the concept in [10], defined the following multi-valued mapping $\partial_{\text{HS}}\mathbf{x}(\mathbf{b}): \mathbb{R}^n \rightrightarrows \mathbb{R}^{n \times n}$:

$$\partial_{\text{HS}}\mathbf{x}(\mathbf{b}) := \left\{ \begin{array}{l} P \in \mathbb{R}^{n \times n} \mid P = Q^{-1} - Q^{-1}A(K)Q^{-1}, \\ K \in \mathcal{K}(\mathbf{b}) \end{array} \right\} \quad (9)$$

as a computational replacement for $\partial_B\mathbf{x}(\mathbf{b})$, where

$$A(K) = C_K^T (C_K Q^{-1} C_K^T)^{-1} C_K.$$

The set $\partial_{\text{HS}}\mathbf{x}(\mathbf{b})$ is known as the HS-Jacobian of $\mathbf{x}(\cdot)$ at \mathbf{b} . However, checking whether a matrix is full rank is a challenging and costly task, especially for large scale matrices. Fortunately, the following proposition from [14] provides a computationally efficient way to get an element in $\partial_{\text{HS}}\mathbf{x}(\mathbf{b})$ without the need to check the full rank condition.

Proposition 3 (Proposition 2, [14]) For any $\mathbf{b} \in \mathbb{R}^n$, there exists a neighborhood U of \mathbf{b} such that

$$\mathcal{K}(\mathbf{b}') \subseteq \mathcal{K}(\mathbf{b}), \partial_{\text{HS}\mathbf{x}}(\mathbf{b}') \subseteq \partial_{\text{HS}\mathbf{x}}(\mathbf{b}), \forall \mathbf{b}' \in U.$$

If $\mathcal{K}(\mathbf{b}') \subseteq \mathcal{K}(\mathbf{b})$, then $\mathbf{x}(\mathbf{b}') = \mathbf{x}(\mathbf{b}) + P(\mathbf{b}' - \mathbf{b}), \forall P \in \partial_{\text{HS}\mathbf{x}}(\mathbf{b}')$. Furthermore, let $I(\mathbf{b})$ be given in (8). Denote

$$\Omega := Q^{-1} - Q^{-1}C_{I(\mathbf{b})}^T(C_{I(\mathbf{b})}Q^{-1}C_{I(\mathbf{b})}^T)^\dagger C_{I(\mathbf{b})}Q^{-1},$$

we have that $\Omega \in \partial_{\text{HS}\mathbf{x}}(\mathbf{b})$.

Based on the results in Proposition 2 and Proposition 3, we can now compute a specific element in the HS-Jacobian $\partial_{\text{HS} \text{Prox}_{\rho \|\cdot\|_1^2}}(\cdot)$ at any $\mathbf{a} \in \mathbb{R}^n$ as described in the following theorem.

Theorem 1 Given $\mathbf{a} \in \mathbb{R}^n$ and $\rho > 0$, let $\Pi \in \mathbb{R}^{n \times n}$ be the permutation matrix such that $\Pi|\mathbf{a}| = \mathbf{b}$ with $\mathbf{b}_1 \geq \mathbf{b}_2 \geq \dots \geq \mathbf{b}_n \geq 0$. Then, the HS-Jacobian $\partial_{\text{HS} \text{Prox}_{\rho \|\cdot\|_1^2}}(\mathbf{a})$ can be given as

$$\partial_{\text{HS} \text{Prox}_{\rho \|\cdot\|_1^2}}(\mathbf{a}) = \{ \Theta \Pi^T P \Pi \Theta \mid P \in \partial_{\text{HS}\mathbf{x}}(\mathbf{b}) \},$$

where $\partial_{\text{HS}\mathbf{x}}(\cdot)$ is defined as in (9) and $\Theta = \text{Diag}(\text{sign}(\mathbf{a}))$. Moreover, $M_0 \in \mathbb{R}^{n \times n}$ given by

$$M_0 := \Theta \Pi^T \Omega \Pi \Theta \tag{10}$$

is an element in the HS-Jacobian $\partial_{\text{HS} \text{Prox}_{\rho \|\cdot\|_1^2}}(\mathbf{a})$, where

$$\Omega = Q^{-1} - Q^{-1}C_{I(\mathbf{b})}^T \left(C_{I(\mathbf{b})}Q^{-1}C_{I(\mathbf{b})}^T \right)^\dagger C_{I(\mathbf{b})}Q^{-1},$$

and the matrices Q and C are defined in (6).

3 A semismooth Newton-CG based augmented Lagrangian method

In this section, we design a semismooth Newton based augmented Lagrangian method (SSNAL) for solving the exclusive lasso model, which is a special case of the two-block convex composite programming problem.

3.1 SSNAL for the exclusive lasso model

Consider the following 2-block convex composite programming problem

$$\min_{\mathbf{x}} F(\mathbf{x}) := f(\mathcal{A}\mathbf{x}) - \langle \mathbf{c}, \mathbf{x} \rangle + p(\mathbf{x}), \tag{11}$$

where $f : \mathbb{R}^m \rightarrow \mathbb{R}$ is a smooth convex function, $p(\cdot) = \lambda \Omega_{EL}^{\mathcal{G}}(\cdot)$, where $\Omega_{EL}^{\mathcal{G}}(\cdot)$ is the exclusive lasso regularizer defined in (1) and $\lambda > 0$ is a parameter; $\mathcal{A} : \mathbb{R}^n \rightarrow \mathbb{R}^m$ is a

linear mapping and $\mathbf{c} \in \mathbb{R}^n$. Due to the discussion in section 2, the proximal mapping $\text{Prox}_{\sigma p}(\cdot)$ can be computed efficiently given any positive scalar σ . To derive the dual problem of (11), we first write (11) equivalently as

$$(P) \min_{\mathbf{x}, \mathbf{y}, \mathbf{z}} \{f(\mathbf{y}) - \langle \mathbf{c}, \mathbf{x} \rangle + p(\mathbf{z}) \mid \mathcal{A}\mathbf{x} - \mathbf{y} = 0, \mathbf{x} - \mathbf{z} = 0\}.$$

The minimization form of the dual of (P) is given by

$$(D) \min_{\mathbf{u}, \mathbf{v}} \{f^*(\mathbf{u}) + p^*(\mathbf{v}) \mid \mathcal{A}^*\mathbf{u} + \mathbf{v} - \mathbf{c} = 0\},$$

where $f^*(\cdot)$ and $p^*(\cdot)$ are the conjugate functions of f and p , respectively. Define the Lagrangian function for (D) as

$$l(\mathbf{u}, \mathbf{v}; \mathbf{x}) = f^*(\mathbf{u}) + p^*(\mathbf{v}) - \langle \mathbf{x}, \mathcal{A}^*\mathbf{u} + \mathbf{v} - \mathbf{c} \rangle.$$

Assume that $f^*(\cdot)$ is twice continuously differentiable and strongly convex in $\text{int}(\text{dom}(f^*))$. Then the KKT conditions for (D) are given as follows:

$$(KKT) \quad \begin{cases} \nabla f^*(\mathbf{u}) - \mathcal{A}\mathbf{x} = 0, \\ \mathbf{v} - \text{Prox}_{p^*}(\mathbf{v} + \mathbf{x}) = 0, \\ \mathcal{A}^*\mathbf{u} + \mathbf{v} - \mathbf{c} = 0. \end{cases}$$

Now, we introduce the SSNAL for solving (D), which will also solve the primal problem (P) as a by-product.

For a given parameter $\sigma > 0$, the augmented Lagrangian function associated with (D) is given by

$$\mathcal{L}_\sigma(\mathbf{u}, \mathbf{v}; \mathbf{x}) = l(\mathbf{u}, \mathbf{v}; \mathbf{x}) + \frac{\sigma}{2} \|\mathcal{A}^*\mathbf{u} + \mathbf{v} - \mathbf{c}\|_2^2.$$

We present the SSNAL algorithm for solving (D) in Algorithm 1. To guarantee the

Algorithm 1 SSNAL for (D)

Initialization: Choose $(\mathbf{u}^0, \mathbf{v}^0, \mathbf{x}^0) \in \text{int}(\text{dom}(f^*)) \times \text{dom}(p^*) \times \mathbb{R}^n$, $\sigma_0 > 0$ and a summable nonnegative sequence $\{\epsilon_k\}$.

repeat

Step 1. Compute

$$(\mathbf{u}^{k+1}, \mathbf{v}^{k+1}) \approx \arg \min \{\Phi_k(\mathbf{u}, \mathbf{v}) = \mathcal{L}_{\sigma_k}(\mathbf{u}, \mathbf{v}; \mathbf{x}^k)\} \quad (12)$$

 to satisfy the condition (A) with the tolerance ϵ_k .

Step 2. Update $\mathbf{x}^{k+1} = \mathbf{x}^k - \sigma_k(\mathcal{A}^*\mathbf{u}^{k+1} + \mathbf{v}^{k+1} - \mathbf{c})$.

Step 3. Update $\sigma_{k+1} \uparrow \sigma_\infty \leq \infty$.

until Stopping criterion is satisfied.

convergence of the inexact augmented Lagrangian method (ALM), we need the following stopping criterion for solving the subproblem (12):

$$(A) \quad \text{dist}(0, \partial\Phi_k(\mathbf{u}^{k+1}, \mathbf{v}^{k+1})) \leq \epsilon_k / \max\{1, \sqrt{\sigma_k}\}.$$

The inexact ALM is a well established algorithmic framework for solving convex programming problems [22, 23]. The key challenge in executing the inexact ALM is whether the nonsmooth problem (12) can be solved efficiently. In this paper, we design a semismooth Newton (SSN) method to solve (12) that can achieve a superlinear (or even quadratic) convergence rate. We should emphasize that the efficiency in computing the Newton direction in each SSN iteration depending critically on exploiting the sparse structure of the generalized Hessian of the underlying nonsmooth function which in turns relies on the structure of the elements of the HS-Jacobian $\partial_{\text{HS}}\text{Prox}_{\sigma kp}(\cdot)$. Now, we describe how to solve the subproblem (12).

3.2 A semismooth Newton method for solving (12)

For a given $\sigma > 0$, the subproblem (12) in each iteration of Algorithm 1 is given by

$$\min_{\mathbf{u}, \mathbf{v}} \Phi(\mathbf{u}, \mathbf{v}) = \mathcal{L}_\sigma(\mathbf{u}, \mathbf{v}; \tilde{\mathbf{x}}). \quad (13)$$

Since $\Phi(\mathbf{u}, \mathbf{v})$ is strongly convex, (13) admits a unique optimal solution which we denote as $(\bar{\mathbf{u}}, \bar{\mathbf{v}})$. Now, for any \mathbf{u} , denote

$$\begin{aligned} \phi(\mathbf{u}) &:= \inf_{\mathbf{v}} \Phi(\mathbf{u}, \mathbf{v}) \\ &= f^*(\mathbf{u}) + p^*(\text{Prox}_{p^*/\sigma}(\tilde{\mathbf{x}}/\sigma + \mathbf{c} - \mathcal{A}^*\mathbf{u})) \\ &\quad + \frac{1}{2\sigma} \|\text{Prox}_{\sigma p}(\tilde{\mathbf{x}} + \sigma\mathbf{c} - \sigma\mathcal{A}^*\mathbf{u})\|^2 - \frac{1}{2\sigma} \|\tilde{\mathbf{x}}\|^2. \end{aligned} \quad (14)$$

Then, we can solve for $(\bar{\mathbf{u}}, \bar{\mathbf{v}})$ simultaneously as

$$\bar{\mathbf{u}} = \arg \min_{\mathbf{u}} \phi(\mathbf{u}), \quad \bar{\mathbf{v}} = \text{Prox}_{p^*/\sigma}(\tilde{\mathbf{x}}/\sigma + \mathbf{c} - \mathcal{A}^*\bar{\mathbf{u}}).$$

Since $\phi(\cdot)$ is strongly convex and continuously differentiable with

$$\nabla \phi(\mathbf{u}) = \nabla f^*(\mathbf{u}) - \mathcal{A} \text{Prox}_{\sigma p}(\tilde{\mathbf{x}} + \sigma\mathbf{c} - \sigma\mathcal{A}^*\mathbf{u}),$$

we know that $\bar{\mathbf{u}}$ can be obtained by solving the following nonlinear and nonsmooth equation

$$\nabla \phi(\mathbf{u}) = 0. \quad (15)$$

Due to the quadratic convergence of Newton's method, it is usually the first choice for solving nonlinear equations if it can be efficiently implemented. However, the direct application of Newton's method to (15) is not feasible since the function $\nabla \phi(\cdot)$ is nonsmooth. Fortunately, the semismooth version of the Newton's method has been established in [12, 19]. This allows us to solve (15) by a semismooth Newton method, which has at least the superlinear convergence property. The concept of semismoothness can be found in the appendices.

Remark 2 Note that all finite-valued convex functions are semismooth [17]. Since $\text{Prox}_{\sigma p}(\cdot)$ is piecewise linear and Lipschitz continuous, it is directionally differentiable

[8]. And from Proposition 3, we can obtain that there exists a neighborhood \mathcal{X} of \mathbf{a} such that for all $\mathbf{a}' \in \mathcal{X}$,

$$\text{Prox}_{\sigma\rho\|\cdot\|_1^2}(\mathbf{a}') - \text{Prox}_{\sigma\rho\|\cdot\|_1^2}(\mathbf{a}) - M(\mathbf{a}' - \mathbf{a}) = 0,$$

for any $M \in \partial_{\text{HS}}\text{Prox}_{\sigma\rho\|\cdot\|_1^2}(\mathbf{a}')$. Thus $\text{Prox}_{\sigma\rho}(\cdot)$ is strongly semismooth with respect to $\partial_{\text{HS}}\text{Prox}_{\sigma\rho\|\cdot\|_1^2}(\cdot)$.

We now derive the generalized Jacobian of the locally Lipschitz function $\nabla\phi(\cdot)$. For a given \mathbf{u} , the following set-valued map is well defined:

$$\hat{\partial}^2\phi(\mathbf{u}) := \nabla^2 f^*(\mathbf{u}) + \sigma\mathcal{A}\partial_{\text{HS}}\text{Prox}_{\sigma\rho}(\tilde{\mathbf{x}} + \sigma\mathbf{c} - \sigma\mathcal{A}^*\mathbf{u})\mathcal{A}^*,$$

where $\partial_{\text{HS}}\text{Prox}_{\sigma\rho}(\tilde{\mathbf{x}} + \sigma\mathbf{c} - \sigma\mathcal{A}^*\mathbf{u})$ is the HS-Jacobian of the Lipschitz continuous mapping $\text{Prox}_{\sigma\rho}(\cdot)$ at $\tilde{\mathbf{x}} + \sigma\mathbf{c} - \sigma\mathcal{A}^*\mathbf{u}$.

Now, we present our semismooth Newton-CG (SSNCG) method in Algorithm 2 for solving (12) which we can expect to get a fast superlinear (or even quadratic) convergence.

Algorithm 2 SSNCG for (12)

Initialization: Given $\mathbf{u}^0 \in \text{int}(\text{dom}(f^*))$, $\mu \in (0, 1/2)$, $\tau \in (0, 1]$, and $\bar{\gamma}, \delta \in (0, 1)$. For $j = 0, 1, 2, \dots$

repeat

Step 1. Select an element $\mathcal{H}_j \in \hat{\partial}^2\phi(\mathbf{u}^j)$. Apply the conjugate gradient (CG) method to find an approximate solution $\mathbf{d}^j \in \mathbb{R}^m$ to

$$\mathcal{H}_j(\mathbf{d}^j) \approx -\nabla\phi(\mathbf{u}^j) \tag{16}$$

such that

$$\|\mathcal{H}_j(\mathbf{d}^j) + \nabla\phi(\mathbf{u}^j)\| \leq \min(\bar{\eta}, \|\nabla\phi(\mathbf{u}^j)\|^{1+\tau}).$$

Step 2. (Line search) Set $\alpha_j = \delta^{m_j}$, where m_j is the first nonnegative integer m for which

$$\phi(\mathbf{u}^j + \delta^m \mathbf{d}^j) \leq \phi(\mathbf{u}^j) + \mu\delta^m \langle \nabla\phi(\mathbf{u}^j), \mathbf{d}^j \rangle.$$

Step 3. Set $\mathbf{u}^{j+1} = \mathbf{u}^j + \alpha_j \mathbf{d}^j$.

until Stopping criterion based on $\|\nabla\phi(\mathbf{u}^{j+1})\|$ is satisfied.

3.3 Convergence results

In this subsection, we show the convergence of our proposed algorithms SSNAL and SSNCG. The convergence rate of the two algorithms have been well studied in [37, 13]. We adopt the results here for the convenience of the readers. The detailed statement and proof of the theorems could be found in the appendices [37, 13].

Theorem 2 Assume that the solution set Ω to (11) is nonempty.

(1) Let $\{(\mathbf{u}^k, \mathbf{v}^k, \mathbf{x}^k)\}$ be the sequence generated by Algorithm 1 with the stopping criterion (A). Then the sequence $\{(\mathbf{u}^k, \mathbf{v}^k)\}$ converges to the unique optimal solution of (D), and $\|\mathcal{A}^* \mathbf{u}^k + \mathbf{v}^k - \mathbf{c}\|$ converges to zero. In addition, $\{\mathbf{x}^k\}$ converges to an optimal solution of (P).

(2) Assume $\mathcal{T}_F(\mathbf{x}) = \partial F(\mathbf{x})$ satisfies the error bound condition with modulus a_F . If $\{(\mathbf{u}^k, \mathbf{v}^k, \mathbf{x}^k)\}$ is generated by Algorithm 1 with the stopping criteria (A) and (B), where for a given summable nonnegative sequence $\{\delta_k\}$, stopping criterion (B) is defined as

$$\text{dist}(0, \partial \Phi_k(\mathbf{u}^{k+1}, \mathbf{v}^{k+1})) \leq \delta_k \sqrt{\sigma_k} \|\mathcal{A}^* \mathbf{u}^{k+1} + \mathbf{v}^{k+1} - \mathbf{c}\|.$$

Then one have that for k sufficiently large,

$$\text{dist}(\mathbf{x}^{k+1}, \Omega) \leq \theta_k \text{dist}(\mathbf{x}^k, \Omega),$$

where $\theta_k = (a_F(a_F^2 + \sigma_k^2)^{-1/2} + 2\delta_k)(1 - \delta_k)^{-1} \rightarrow \theta_\infty = a_F(a_F^2 + \sigma_\infty^2)^{-1/2} < 1$ as $k \rightarrow +\infty$.

Theorem 3 Let the sequence $\{\mathbf{u}^j\}$ be generated by Algorithm 2. Then $\{\mathbf{u}^j\}$ converges to the unique solution $\bar{\mathbf{u}}$ of the problem in (14), and for j sufficiently large,

$$\|\mathbf{u}^{j+1} - \bar{\mathbf{u}}\| = O(\|\mathbf{u}^j - \bar{\mathbf{u}}\|^{1+\tau}),$$

where $\tau \in (0, 1]$ is a given constant in the algorithm, which is typically chosen to be 0.5 in our experiments.

4 Numerical experiments

With our derived closed-form solution for $\text{Prox}_{\rho\|\cdot\|_1^2}$ and its HS-Jacobian $\partial_{\text{HS}} \text{Prox}_{\rho\|\cdot\|_1^2}(\cdot)$, we can solve the following exclusive lasso model [3] using our proposed algorithmic framework SSNAL:

$$\min_{\mathbf{x}} \frac{1}{2} \|\mathbf{A}\mathbf{x} - \mathbf{b}\|_2^2 + \lambda \sum_{g \in \mathcal{G}} \|\mathbf{x}_g\|_1^2, \quad (17)$$

where $\mathcal{G} = \{g \mid g \subseteq \{1, 2, \dots, n\}\}$ is a disjoint partition of $\{1, 2, \dots, n\}$. By taking $f(x) = \frac{1}{2} \|\mathbf{x} - \mathbf{b}\|_2^2$, $\mathbf{c} = 0$, we can reformulate (17) in the form of (11). Thus, all the analysis in previous sections is applicable for the above model.

In the numerical experiments, we mainly focus on two aspects. (1) We compare our proposed SSNAL to two popular state-of-the-art first-order frameworks, ADMM and APG, for solving (17). To demonstrate the efficiency and scalability of our proposed SSNAL, we perform the time comparison on synthetic datasets from small to large scales. (2) We apply the exclusive lasso model (17) to the partial index tracking problem in finance. The out-of-sample results show the superior performance of the exclusive lasso model in index tracking, comparing to the lasso model. All our computational results are obtained by running MATLAB on a windows workstation (12-core, Intel Xeon E5-2680 @

2.50GHz, 128G RAM). We stop all the three algorithms by the following criterion based on the relative KKT residual:

$$\eta_{\text{KKT}} := \frac{\|\mathbf{x} - \text{Prox}_p(\mathbf{x} - A^T(A\mathbf{x} - \mathbf{b}))\|}{1 + \|\mathbf{x}\| + \|A^T(A\mathbf{x} - \mathbf{b})\|} \leq \epsilon,$$

where $\epsilon > 0$ is a given tolerance, which is set to **1e-6** in our experiments. We observed that ADMM and APG are very time consuming for large scale instances. Thus, we also terminate ADMM and APG when they reach the maximum iterations of **2e4** and **1e5**, respectively.

4.1 Synthetic data

In this subsection, we test the efficiency of our proposed second-order based algorithm SSNAL for solving the exclusive lasso model (17), and compare it against ADMM and APG on simulated datasets. We adopt the design of synthetic datasets described in [3]. The numerical results demonstrate the superior performance of SSNAL for solving (17), from small to large scale instances. Here we focus on the time comparison among the algorithms. For the comparison of prediction error among the exclusive lasso, lasso and other linear regression models, we refer the readers to [3] for more details.

In the experiments, we generate the synthetic data using the model $\mathbf{y} = A\mathbf{x}^* + \boldsymbol{\epsilon}$, where \mathbf{x}^* is the predefined true parameter and $\boldsymbol{\epsilon} \in \mathbb{R}^m \sim \mathcal{N}(\mathbf{0}, I_m)$ is a random noise vector. Now, we describe the design of the randomly generated matrix $A \in \mathbb{R}^{m \times np}$. For given integers m , n and p , we generate each row of A by sampling a vector from a multivariate normal distribution $\mathcal{N}(\mathbf{0}, \Sigma)$. We group the features into n groups with p features in each group. Then, we select Σ as a Toeplitz covariance matrix with entries $\Sigma_{ij} = w_1^{|i-j|}$ for features in the same group, and $\Sigma_{ij} = w_2^{|i-j|}$ for features in different groups. In our experiments, we generate two kinds of covariance matrices. The first covariance matrix with $w_1 = w_2 = 0.9$ simulates the high correlation in both between groups and within groups. In the second matrix, we select $w_1 = 0.9$ and $w_2 = 0.3$. Here we mainly focus on feature selection by the exclusive lasso model in the high-dimensional settings. Hence, in our experiments, we fix the number of observations m to be 200. We also fix the number of groups n to be 20, but vary the number of features p in each group from 50 to 2500. That is, we vary the total number of features np from 1000 to 50000. For the ground-truth \mathbf{x}^* , we randomly generate 10 nonzero elements i.i.d from Uniform(0, 10) in each group.

To compare the robustness of different algorithms with respect to the hyperparameter λ , we test all the algorithms under two widely different values of λ . Selected numerical results are shown in Figure 1, which demonstrate the superior performance of SSNAL, especially for large scale instances, comparing to ADMM and APG. In addition, we run another experiment under the second setting of covariance matrix, and take $\lambda = 0.1$, $np = 100000$, SSNAL only takes 122 seconds to successfully solve it. More numerical results could be found in the appendices. The power of SSNAL for solving large scale problems also shows the importance of the analytical result derived for the special element M_0 of the HS-Jacobian $\partial_{\text{HS}} \text{Prox}_{\rho, \|\cdot\|_1^2}(\cdot)$.

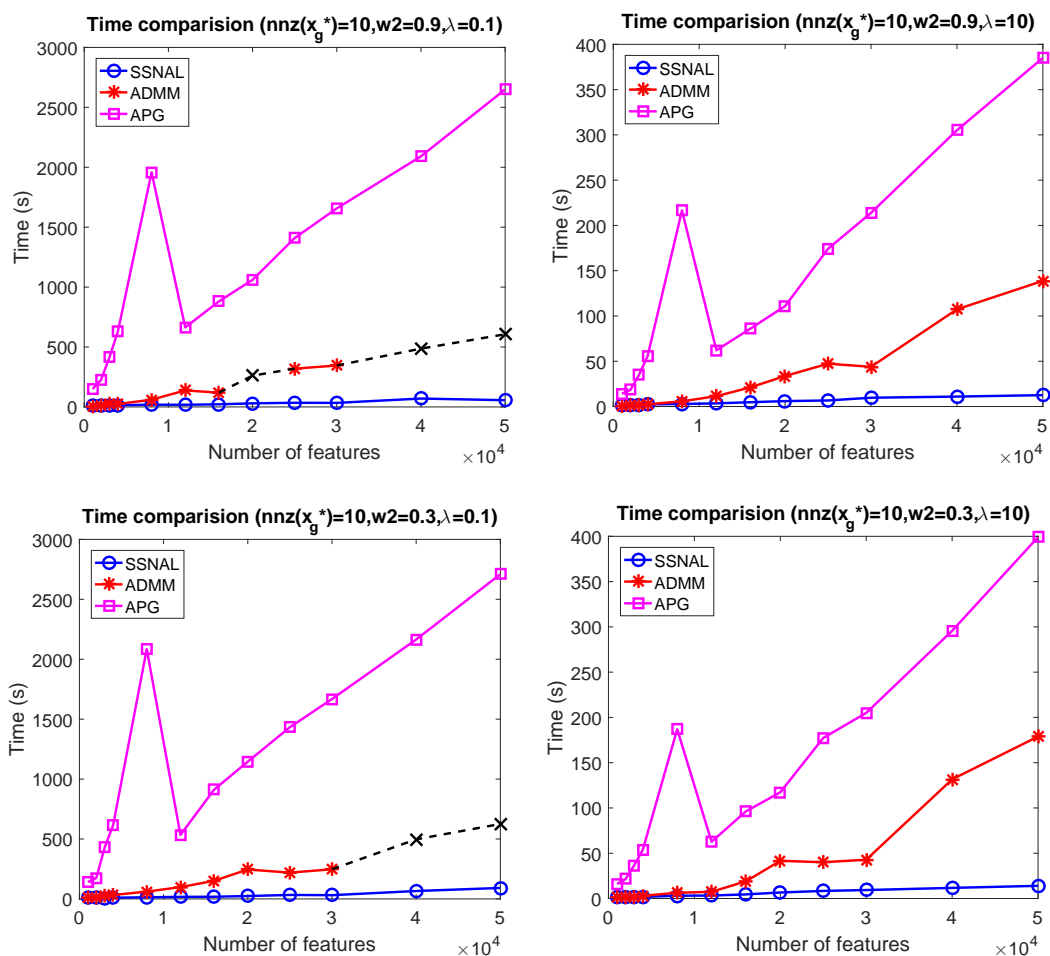


Figure 1: Time comparison among SSNAL, ADMM and APG on synthetic datasets. The black dash line with "x" represents that the algorithm fails to solve the instance while the maximum iteration is reached. $\text{nnz}(x_g)$ means the number of non-zeros in each group of x^* .

4.2 Partial index tracking

In this subsection, we apply the exclusive lasso model in a real application in finance. Consider the portfolio selection problem where a fund manager wants to select a small subset of stocks (to minimize transaction costs and business analyses) to track a target time series such as the S&P 500 index. Furthermore, in order to diversify the risks, the portfolio is required to span across all sectors. Such a problem naturally leads us to consider the exclusive lasso model for this application.

In our experiments, we download all stock price data in the US market between 2018-01-01 and 2018-12-31 (251 trading days) from Yahoo finance [1]. We drop the stock if

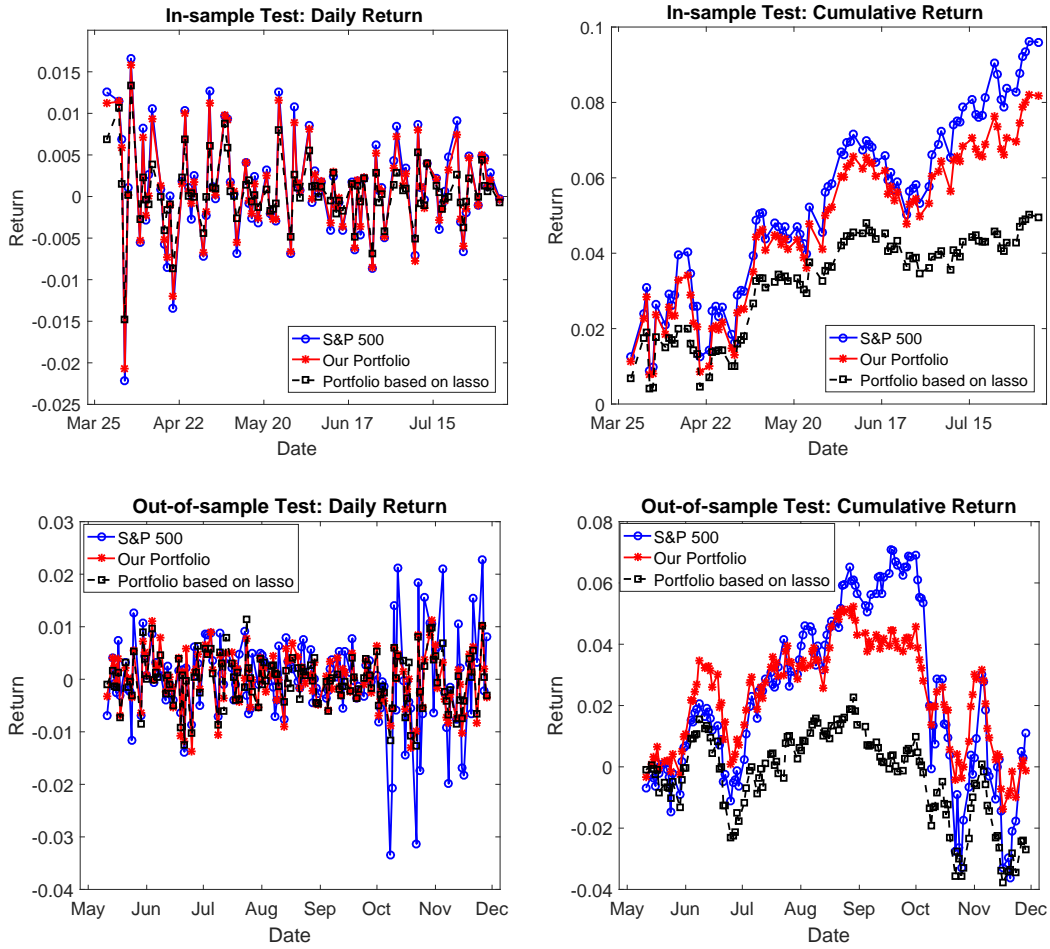


Figure 2: In-sample and out-of-sample performance of exclusive lasso model and lasso model for partial index tracking of S&P 500.

10% of its price data is missing. After that, we get 3074 stocks in our stock universe. For the remaining stocks, we handle the missing data via the common practice of forward interpolation. We then compute the daily return and get the historical return matrix $R \in \mathbb{R}^{250 \times 3074}$. We try to build a portfolio to track the popular S&P 500 index. Let $\mathbf{y} \in \mathbb{R}^{250}$ be the daily return of the S&P 500 index in 2018. Since there are 12 sectors in the US market (e.g., finance, healthcare, technology, etc.), we have a natural group partition for our stock universe as $\mathcal{G}_{US} = \{g_1, g_2, \dots, g_{12}\}$, where g_i is the index set for stocks in the i -th sector.

To test the performance of the exclusive lasso model in partial index tracking, we use the rolling window method to test the in-sample and out-of-sample performance of the model. We use the historical data in the last 90 trading days to estimate a weight vector

via the model for the future 10 days. More specifically, at day T , we solve the following²:

$$\mathbf{x}_T^* = \arg \min_{\mathbf{x}} \frac{1}{2} \|R_T \mathbf{x} - \mathbf{y}_T\|_2^2 + \lambda_T \sum_{g \in \mathcal{G}_{US}} \|\mathbf{x}_g\|_1,$$

where R_T , \mathbf{y}_T are the daily return matrix of all stocks in our stock universe and S&P 500 index in the last 90 trading days prior to day T , respectively. We select the hyper-parameter λ_T using 9-folds cross validation. After we get the estimated weight vector \mathbf{x}_T^* , we invest in the market based on it for the next 10 trading days. The in-sample and out-of-sample performance of the exclusive lasso model and the lasso model are shown in Figure 2. For in-sample performance, we just show the selected results of one rolling window. The performance demonstrates the viability of using the exclusive lasso model in partial index tracking by selecting a small subset of about 60 stocks from the large universe of 3074 stocks. Furthermore, we plot the percentage of stocks from each sector

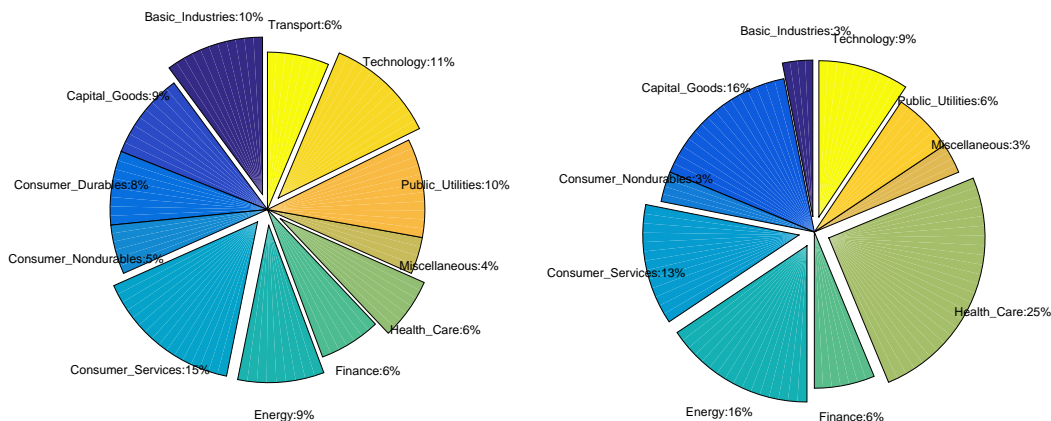


Figure 3: Percentage of selected stocks by sectors. Left: exclusive lasso model. Right: lasso model.

in the portfolio obtained from our exclusive lasso model and the lasso model in Figure 3. The result shows that our exclusive lasso model can select stocks from all the 12 sectors but the lasso model selects stocks only from 10 sectors in the universe. More comparison between the exclusive lasso and lasso model in partial index tracking could be found in the appendices.

5 Conclusion

In this paper, we derive the closed-form solution for $\text{Prox}_{\rho\|\cdot\|_1^2}(\cdot)$ and its HS-Jacobian. Based on these new theoretical results, we design an efficient and scalable second-order based algorithm SSNAL to solve the exclusive lasso model. We then apply the exclusive lasso model in partial index tracking, which achieved better out-of-sample performance

²We explain why we could drop the constraints: $\mathbf{x} \geq 0$ and $\sum_i \mathbf{x}_i = 1$ in the appendices.

comparing to the lasso model. For future work, as motivated by the superior performance of the exclusive lasso regularizer and our proposed algorithm SSNAL on regression problems, we plan to generalize the results to classification problems, replacing the smooth least square loss function by the nonsmooth softmax loss function.

References

- [1] *Yahoo Finance*: <https://finance.yahoo.com>.
- [2] A. BECK AND M. TEBoulLE, *A fast iterative shrinkage-thresholding algorithm for linear inverse problems*, SIAM J. Imaging Sciences, 2 (2009), pp. 183–202.
- [3] F. CAMPBELL AND G. I. ALLEN, *Within group variable selection through the exclusive lasso*, Electronic J. of Statistics, 11 (2017), pp. 4220–4257.
- [4] E. CANDÉS AND T. TAO, *The dantzig selector: Statistical estimation when p is much larger than n* , The Annals of Statistics, 35 (2007), pp. 2313–2351.
- [5] S. S. CHEN, D. L. DONOHO, AND M. A. SAUNDERS, *Atomic decomposition by basis pursuit*, SIAM Review, 43 (2001), pp. 129–159.
- [6] J. ECKSTEIN AND D. P. BERTSEKAS, *On the Douglas-Rachford splitting method and the proximal point algorithm for maximal monotone operators*, Mathematical Programming, 55 (1992), pp. 293–318.
- [7] B. EFRON, T. HASTIE, I. JOHNSTONE, AND R. TIBSHIRANI, *Least angle regression*, The Annals of Statistics, 32 (2004), pp. 407–499.
- [8] F. FACCHINEI AND J.-S. PANG, *Finite-dimensional variational inequalities and complementarity problems*, Springer Science & Business Media, 2007.
- [9] R. GLOWINSKI AND A. MARROCO, *Sur l’approximation, par éléments finis d’ordre un, et la résolution, par pénalisation-dualité d’une classe de problèmes de dirichlet non linéaires*, Revue française d’automatique, informatique, recherche opérationnelle. Analyse numérique, 9 (1975), pp. 41–76.
- [10] J. HAN AND D. F. SUN, *Newton and quasi-Newton methods for normal maps with polyhedral sets*, J. Optimization Theory and Applications, 94 (1997), pp. 659–676.
- [11] D. KONG, R. FUJIMAKI, J. LIU, F. NIE, AND C. DING, *Exclusive feature learning on arbitrary structures via $l_{1,2}$ -norm*, in Advances in Neural Information Processing Systems, 2014, pp. 1655–1663.
- [12] B. KUMMER, *Newton’s method for non-differentiable functions*, Advances in Mathematical Optimization, 45 (1988), pp. 114–125.

- [13] X. LI, D. F. SUN, AND K.-C. TOH, *A highly efficient semismooth Newton augmented Lagrangian method for solving Lasso problems*, SIAM J. Optimization, 28 (2018), pp. 433–458.
- [14] ———, *On efficiently solving the subproblems of a level-set method for fused lasso problems*, SIAM J. Optimization, 28 (2018), pp. 1842–1866.
- [15] M. LIN, Y.-J. LIU, D. F. SUN, AND K.-C. TOH, *Efficient sparse Hessian based algorithms for the clustered lasso problem*, arXiv preprint arXiv:1808.07181, (2018).
- [16] F. J. LUQUE, *Asymptotic convergence analysis of the proximal point algorithm*, SIAM Journal on Control and Optimization, 22 (1984), pp. 277–293.
- [17] R. MIFFLIN, *Semismooth and semiconvex functions in constrained optimization*, SIAM J. Control and Optimization, 15 (1977), pp. 959–972.
- [18] Y. NESTEROV, *Gradient methods for minimizing composite functions*, Mathematical Programming, 140 (2013), pp. 125–161.
- [19] L. QI AND J. SUN, *A nonsmooth version of Newton’s method*, Mathematical Programming, 58 (1993), pp. 353–367.
- [20] S. M. ROBINSON, *Some continuity properties of polyhedral multifunctions*, in Mathematical Programming at Oberwolfach, Springer, 1981, pp. 206–214.
- [21] R. T. ROCKAFELLAR, *Convex Analysis*, Princeton University Press, 1970.
- [22] R. T. ROCKAFELLAR, *Augmented Lagrangians and applications of the proximal point algorithm in convex programming*, Mathematics of Operations Research, 1 (1976), pp. 97–116.
- [23] ———, *Monotone operators and the proximal point algorithm*, SIAM J. Control and Optimization, 14 (1976), pp. 877–898.
- [24] J. SUN, *On monotropic piecewise quadratic programming*, PhD thesis, University of Washington, 1986.
- [25] R. TIBSHIRANI, *Regression shrinkage and selection via the lasso*, J. of the Royal Statistical Society: Series B, (1996), pp. 267–288.
- [26] R. TIBSHIRANI, M. SAUNDERS, S. ROSSET, J. ZHU, AND K. KNIGHT, *Sparsity and smoothness via the fused lasso*, J. of the Royal Statistical Society: Series B, 67 (2005), pp. 91–108.
- [27] A. WANG, J. CAI, J. LU, AND T.-J. CHAM, *Structure-aware multimodal feature fusion for RGB-D scene classification and beyond*, ACM Transactions on Multimedia Computing, Communications, and Applications, 14 (2018), p. 39.

- [28] Y. WANG, J. YANG, W. YIN, AND Y. ZHANG, *A new alternating minimization algorithm for total variation image reconstruction*, SIAM J. Imaging Sciences, 1 (2008), pp. 248–272.
- [29] M. YAMADA, T. KOH, T. IWATA, J. SHAWE-TAYLOR, AND S. KASKI, *Localized lasso for High-Dimensional Regression*, in Artificial Intelligence and Statistics, 2017, pp. 325–333.
- [30] J. YOON AND S. J. HWANG, *Combined group and exclusive sparsity for deep neural networks*, in International Conference on Machine Learning, 2017, pp. 3958–3966.
- [31] L. YUAN, J. LIU, AND J. YE, *Efficient methods for overlapping group lasso*, in Advances in Neural Information Processing Systems, 2011, pp. 352–360.
- [32] M. YUAN AND Y. LIN, *Model selection and estimation in regression with grouped variables*, J. of the Royal Statistical Society: Series B, 68 (2006), pp. 49–67.
- [33] Y. YUAN, D. F. SUN, AND K.-C. TOH, *An efficient semismooth Newton based algorithm for convex clustering*, in Proceedings of the 35th International Conference on Machine Learning, 2018, pp. 5718–5726.
- [34] T. ZHANG, B. GHANEM, S. LIU, C. XU, AND N. AHUJA, *Robust visual tracking via exclusive context modeling*, IEEE Transactions on Cybernetics, 46 (2016), pp. 51–63.
- [35] Y. ZHANG, N. ZHANG, D. F. SUN, AND K.-C. TOH, *An efficient Hessian based algorithm for solving large-scale sparse group lasso problems*, Mathematical Programming, (2018).
- [36] P. ZHAO AND B. YU, *On model selection consistency of lasso*, J. of Machine Learning Research, 7 (2006), pp. 2541–2563.
- [37] X.-Y. ZHAO, D. F. SUN, AND K.-C. TOH, *A Newton-CG augmented Lagrangian method for semidefinite programming*, SIAM J. Optimization, 20 (2010), pp. 1737–1765.
- [38] Y. ZHOU, R. JIN, AND S. C.-H. HOI, *Exclusive lasso for multi-task feature selection*, in Proceedings of the Thirteenth International Conference on Artificial Intelligence and Statistics, 2010, pp. 988–995.
- [39] H. ZOU, *The adaptive lasso and its oracle properties*, J. of the American Statistical Association, 101 (2006), pp. 1418–1429.

Appendices

A Definition of semismoothness [17, 12, 19]

Definition 1 (*Semismoothness*). For a given open set $\mathcal{O} \subseteq \mathbb{R}^n$, let $F : \mathcal{O} \rightarrow \mathbb{R}^m$ be a locally Lipschitz continuous function and $\mathcal{G} : \mathcal{O} \rightrightarrows \mathbb{R}^{m \times n}$ be a nonempty compact valued upper-semicontinuous multifunction. F is said to be semismooth at $\mathbf{x} \in \mathcal{O}$ with respect to the multifunction \mathcal{G} if F is directionally differentiable at x and for any $V \in \mathcal{G}(\mathbf{x} + \Delta\mathbf{x})$ with $\Delta\mathbf{x} \rightarrow 0$,

$$F(\mathbf{x} + \Delta\mathbf{x}) - F(\mathbf{x}) - V\Delta\mathbf{x} = o(\|\Delta\mathbf{x}\|).$$

F is said to be strongly semismooth at $\mathbf{x} \in \mathcal{O}$ with respect to \mathcal{G} if it is semismooth at \mathbf{x} with respect to \mathcal{G} and

$$F(\mathbf{x} + \Delta\mathbf{x}) - F(\mathbf{x}) - V\Delta\mathbf{x} = O(\|\Delta\mathbf{x}\|^2).$$

F is said to be a semismooth (respectively, strongly semismooth) function on \mathcal{O} with respect to \mathcal{G} if it is semismooth (respectively, strongly semismooth) everywhere in \mathcal{O} with respect to \mathcal{G} .

B Details of the convergence results

We show the convergence results of our proposed algorithms SSNAL and SSNCG.

For better understanding, we give the definition of the error bound condition.

Definition 2 (*Error bound*). Let $F : \mathcal{X} \rightrightarrows \mathcal{Y}$ be a multivalued mapping and $y \in \mathcal{Y}$ satisfy $F^{-1}(y) \neq \emptyset$. F is said to satisfy the error bound condition for the point y with modulus $\kappa \geq 0$ if there exists $\varepsilon > 0$ such that if $x \in \mathcal{X}$ with $\text{dist}(y, F(x)) \leq \varepsilon$, then

$$\text{dist}(x, F^{-1}(y)) \leq \kappa \text{dist}(y, F(x)).$$

B.1 Convergence result of Algorithm SSNAL

Theorem 4 Assume that the solution set Ω to the exclusive lasso problem is nonempty. (1) Let $\{(\mathbf{u}^k, \mathbf{v}^k, \mathbf{x}^k)\}$ be the sequence generated by Algorithm SSNAL with the stopping criterion (A). Then the sequence $\{(\mathbf{u}^k, \mathbf{v}^k)\}$ converges to the unique optimal solution of (D), and $\|\mathcal{A}^*\mathbf{u}^k + \mathbf{v}^k - \mathbf{c}\|$ converges to zero. In addition, $\{\mathbf{x}^k\}$ converges to an optimal solution of (P).

(2) Assume $\mathcal{T}_F(\mathbf{x}) = \partial F(\mathbf{x})$ satisfies the error bound condition with modulus α_F . If $\{(\mathbf{u}^k, \mathbf{v}^k, \mathbf{x}^k)\}$ is generated by Algorithm SSNAL with the stopping criteria (A) and (B), where for a given summable nonnegative sequence $\{\delta_k\}$, stopping criterion (B) is defined as

$$\text{dist}(0, \partial\Phi_k(\mathbf{u}^{k+1}, \mathbf{v}^{k+1})) \leq \delta_k \sqrt{\sigma_k} \|\mathcal{A}^*\mathbf{u}^{k+1} + \mathbf{v}^{k+1} - \mathbf{c}\|.$$

Then one have that for k sufficiently large,

$$\text{dist}(\mathbf{x}^{k+1}, \Omega) \leq \theta_k \text{dist}(\mathbf{x}^k, \Omega), \quad (18)$$

where $\theta_k = (a_F(a_F^2 + \sigma_k^2)^{-1/2} + 2\delta_k)(1 - \delta_k)^{-1} \rightarrow \theta_\infty = a_F(a_F^2 + \sigma_\infty^2)^{-1/2} < 1$ as $k \rightarrow +\infty$.

Proof 3 (1) The result can be directly obtained from [22, Theorem 4].

(2) Since \mathcal{T}_F satisfies the error bound condition with modulus a_F , it follows from [16, Theorem 2.1] that (18) holds.

Remark 3 When $f(\mathbf{x}) = \|\mathbf{Ax} - b\|^2/2$, F is a piecewise linear-quadratic function, from [24], \mathcal{T}_F is piecewise polyhedral, thus satisfies the error bound condition [20].

B.2 Convergence result of Algorithm SSNCG

Theorem 5 Let the sequence $\{\mathbf{u}^j\}$ be generated by Algorithm SSNCG. Then $\{\mathbf{u}^j\}$ converges to the unique solution $\bar{\mathbf{u}}$ of $\phi(\mathbf{u}) = 0$ (equation (14) in the paper), and for j sufficiently large,

$$\|\mathbf{u}^{j+1} - \bar{\mathbf{u}}\| = O(\|\mathbf{u}^j - \bar{\mathbf{u}}\|^{1+\tau}),$$

where $\tau \in (0, 1]$ is a given constant in the algorithm, which is typically chosen to be 0.5 in our experiments.

Proof 4 By [37, Proposition 3.3 and Theorem 3.4], we can see that $\{\mathbf{u}^j\}$ converges to the unique solution $\bar{\mathbf{u}}$. Then by mimicking the proof of [14, Theorem 3], we can get the convergence rate of $\{\mathbf{u}^j\}$.

C Numerical results

C.1 More numerical results on the synthetic data

In the paper, we present the numerical results for the scenarios where $\text{nnz}(\mathbf{x}_g^*) = 10$ (the number of non-zeros in each group of the ground-truth parameter \mathbf{x}^* is 10). Here we show more numerical results for the case where $\text{nnz}(\mathbf{x}_g^*) = 1$ in Figure 4.

For better illustration, we show the running time of three algorithms under different settings Table 1 - 8. Red numbers in the tables indicate that the algorithm fails to solve the problem when achieving the maximum iteration number.

Table 1: Results of synthetic datasets with $\text{nnz}(\mathbf{x}_g^*) = 10$, $w_2 = 0.9$, $\lambda = 0.1$. Time is in the format of (minutes:seconds).

| np | 1000 | 2000 | 3000 | 4000 | 8000 | 12000 | 16000 | 20000 | 250000 | 30000 | 40000 | 50000 |
|-------|-------|-------|-------|-------|-------|-------|-------|--------------|--------|-------|--------------|--------------|
| SSNAL | 00:08 | 00:11 | 00:11 | 00:15 | 00:19 | 00:18 | 00:22 | 00:30 | 00:35 | 00:34 | 01:10 | 00:56 |
| ADMM | 00:06 | 00:09 | 00:26 | 00:24 | 01:01 | 02:18 | 01:59 | 04:21 | 05:19 | 05:46 | 08:07 | 10:06 |
| APG | 02:30 | 03:46 | 06:54 | 10:30 | 32:37 | 11:04 | 14:41 | 17:41 | 23:29 | 27:37 | 34:51 | 44:10 |

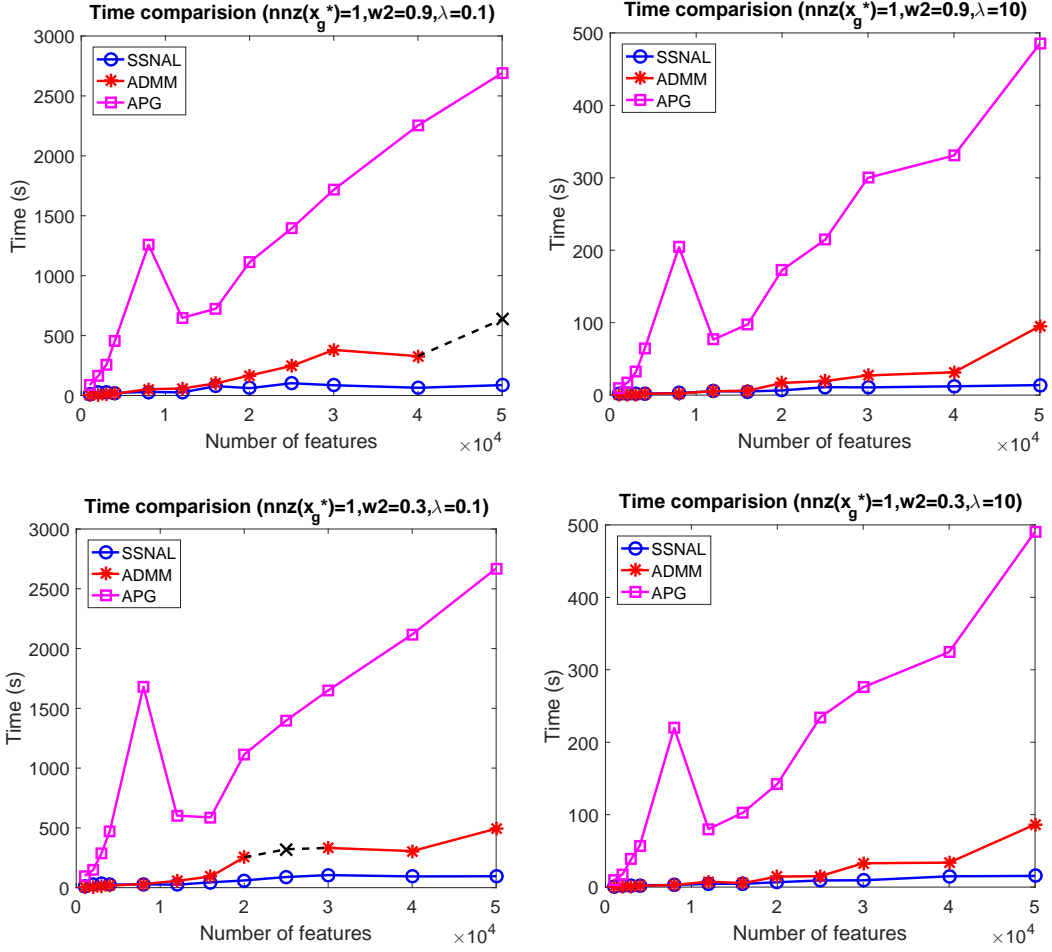


Figure 4: Time comparison among SSNAL, ADMM and APG on synthetic datasets. The black dash line with "x" represents that the algorithm fails to solve the instance while the maximum iteration is reached. $\text{nnz}(\mathbf{x}_g^*)$ means the number of non-zeros in each group of \mathbf{x}^* .

Table 2: Results of synthetic datasets with $\text{nnz}(\mathbf{x}_g^*) = 10$, $w_2 = 0.9$, $\lambda = 10$. Time is in the format of (minutes:seconds).

| np | 1000 | 2000 | 3000 | 4000 | 8000 | 12000 | 16000 | 20000 | 250000 | 30000 | 40000 | 50000 |
|-------|-------|-------|-------|-------|-------|-------|-------|-------|--------|-------|-------|-------|
| SSNAL | 00:01 | 00:02 | 00:02 | 00:02 | 00:03 | 00:03 | 00:05 | 00:06 | 00:07 | 00:10 | 00:11 | 00:13 |
| ADMM | 00:01 | 00:02 | 00:02 | 00:02 | 00:06 | 00:11 | 00:21 | 00:34 | 00:47 | 00:44 | 01:47 | 02:19 |
| APG | 00:14 | 00:18 | 00:35 | 00:56 | 03:37 | 01:02 | 01:26 | 01:51 | 02:54 | 03:34 | 05:05 | 06:25 |

Table 3: Results of synthetic datasets with $\text{nnz}(\mathbf{x}_g^*) = 10$, $w_2 = 0.3$, $\lambda = 0.1$. Time is in the format of (minutes:seconds).

| np | 1000 | 2000 | 3000 | 4000 | 8000 | 12000 | 16000 | 20000 | 250000 | 30000 | 40000 | 50000 |
|-------|-------|-------|-------|-------|-------|-------|-------|-------|--------|-------|-------|-------|
| SSNAL | 00:12 | 00:10 | 00:07 | 00:10 | 00:13 | 00:17 | 00:18 | 00:24 | 00:33 | 00:31 | 01:06 | 01:32 |
| ADMM | 00:09 | 00:13 | 00:26 | 00:33 | 01:01 | 01:39 | 02:31 | 04:05 | 03:39 | 04:07 | 08:17 | 10:25 |
| APG | 02:21 | 02:54 | 07:09 | 10:14 | 34:45 | 08:54 | 15:12 | 19:06 | 23:53 | 27:48 | 36:05 | 45:10 |

Table 4: Results of synthetic datasets with $\text{nnz}(\mathbf{x}_g^*) = 10$, $w_2 = 0.3$, $\lambda = 10$. Time is in the format of (minutes:seconds).

| np | 1000 | 2000 | 3000 | 4000 | 8000 | 12000 | 16000 | 20000 | 250000 | 30000 | 40000 | 50000 |
|-------|-------|-------|-------|-------|-------|-------|-------|-------|--------|-------|-------|-------|
| SSNAL | 00:02 | 00:02 | 00:02 | 00:02 | 00:03 | 00:03 | 00:05 | 00:07 | 00:08 | 00:09 | 00:12 | 00:14 |
| ADMM | 00:01 | 00:02 | 00:01 | 00:03 | 00:06 | 00:07 | 00:19 | 00:42 | 00:40 | 00:43 | 02:12 | 02:59 |
| APG | 00:16 | 00:21 | 00:37 | 00:54 | 03:07 | 01:03 | 01:36 | 01:57 | 02:57 | 03:25 | 04:56 | 06:39 |

Table 5: Results of synthetic datasets with $\text{nnz}(\mathbf{x}_g^*) = 1$, $w_2 = 0.9$, $\lambda = 0.1$. Time is in the format of (minutes:seconds).

| np | 1000 | 2000 | 3000 | 4000 | 8000 | 12000 | 16000 | 20000 | 250000 | 30000 | 40000 | 50000 |
|-------|-------|-------|-------|-------|-------|-------|-------|-------|--------|-------|-------|-------|
| SSNAL | 00:12 | 00:26 | 00:30 | 00:22 | 00:30 | 00:26 | 01:19 | 01:02 | 01:43 | 01:26 | 01:05 | 01:27 |
| ADMM | 00:03 | 00:07 | 00:12 | 00:16 | 00:53 | 00:58 | 01:42 | 02:47 | 04:07 | 06:21 | 05:28 | 10:36 |
| APG | 01:28 | 02:42 | 04:17 | 07:36 | 20:57 | 10:48 | 12:05 | 18:33 | 23:14 | 28:37 | 37:33 | 44:51 |

Table 6: Results of synthetic datasets with $\text{nnz}(\mathbf{x}_g^*) = 1$, $w_2 = 0.9$, $\lambda = 10$. Time is in the format of (minutes:seconds).

| np | 1000 | 2000 | 3000 | 4000 | 8000 | 12000 | 16000 | 20000 | 250000 | 30000 | 40000 | 50000 |
|-------|-------|-------|-------|-------|-------|-------|-------|-------|--------|-------|-------|-------|
| SSNAL | 00:01 | 00:02 | 00:02 | 00:02 | 00:03 | 00:05 | 00:05 | 00:06 | 00:11 | 00:11 | 00:12 | 00:14 |
| ADMM | 00:01 | 00:01 | 00:01 | 00:02 | 00:03 | 00:05 | 00:06 | 00:17 | 00:19 | 00:27 | 00:31 | 00:35 |
| APG | 00:09 | 00:17 | 00:32 | 01:04 | 03:24 | 01:17 | 01:38 | 02:53 | 03:34 | 05:00 | 05:31 | 08:05 |

Table 7: Results of synthetic datasets with $\text{nnz}(\mathbf{x}_g^*) = 1$, $w_2 = 0.3$, $\lambda = 0.1$. Time is in the format of (minutes:seconds).

| np | 1000 | 2000 | 3000 | 4000 | 8000 | 12000 | 16000 | 20000 | 250000 | 30000 | 40000 | 50000 |
|-------|-------|-------|-------|-------|-------|-------|-------|-------|--------|-------|-------|-------|
| SSNAL | 00:10 | 00:24 | 00:35 | 00:25 | 00:28 | 00:25 | 00:44 | 01:00 | 01:29 | 01:45 | 01:34 | 01:35 |
| ADMM | 00:03 | 00:07 | 00:11 | 00:17 | 00:30 | 00:57 | 01:33 | 04:14 | 05:21 | 05:32 | 05:06 | 08:13 |
| APG | 00:10 | 00:18 | 00:39 | 00:57 | 03:40 | 01:20 | 01:43 | 02:22 | 03:54 | 04:36 | 05:24 | 08:11 |

Table 8: Results of synthetic datasets with $\text{nnz}(\mathbf{x}_g^*) = 1$, $w_2 = 0.3$, $\lambda = 10$. Time is in the format of (minutes:seconds).

| np | 1000 | 2000 | 3000 | 4000 | 8000 | 12000 | 16000 | 20000 | 250000 | 30000 | 40000 | 50000 |
|-------|-------|-------|-------|-------|-------|-------|-------|-------|--------|-------|-------|-------|
| SSNAL | 00:01 | 00:02 | 00:02 | 00:02 | 00:03 | 00:05 | 00:05 | 00:07 | 00:09 | 00:09 | 00:15 | 00:15 |
| ADMM | 00:01 | 00:01 | 00:01 | 00:02 | 00:03 | 00:07 | 00:05 | 00:15 | 00:15 | 00:33 | 00:34 | 01:26 |
| APG | 01:39 | 02:26 | 04:45 | 07:54 | 27:59 | 10:03 | 09:48 | 18:34 | 23:19 | 27:29 | 35:18 | 44:30 |

C.2 The explanation of the model of the partial index tracking

In this subsection, we explain why we can drop the simplex constraint $\mathbf{x} \geq 0$, $\sum_i \mathbf{x}_i = 1$ in the partial index tracking application. We assume that we can short stocks in the market, which means we can drop the nonnegative constraint $\mathbf{x} \geq 0$.

Furthermore, we assume the interest rate is r_C . Then, for a given return vector $\mathbf{r} \in \mathbb{R}^n$ of n stocks and a weight vector \mathbf{x}^* , the return of the whole investment is given

by

$$\mathbf{r}^T \mathbf{x}^* + (1 - \sum_{i=1}^n \mathbf{x}_i^*) * r_C = \sum_{i=1}^n (\mathbf{r}_i - r_C) \mathbf{x}_i^* + r_C.$$

Then, if we assume $r_C = 0$, or, we set

$$R = R - r_C, \quad \mathbf{y} = \mathbf{y} - r_C,$$

we could drop the constraint $\sum_{i=1}^n \mathbf{x}_i = 1$ in the index tracking model.

C.3 More results in partial index tracking

In this subsection, we show the in-sample performance of two models over another two rolling windows in Figure 5 and Figure 6. Besides, the percentages of stocks from each sector in the portfolios obtained by two models are also shown.

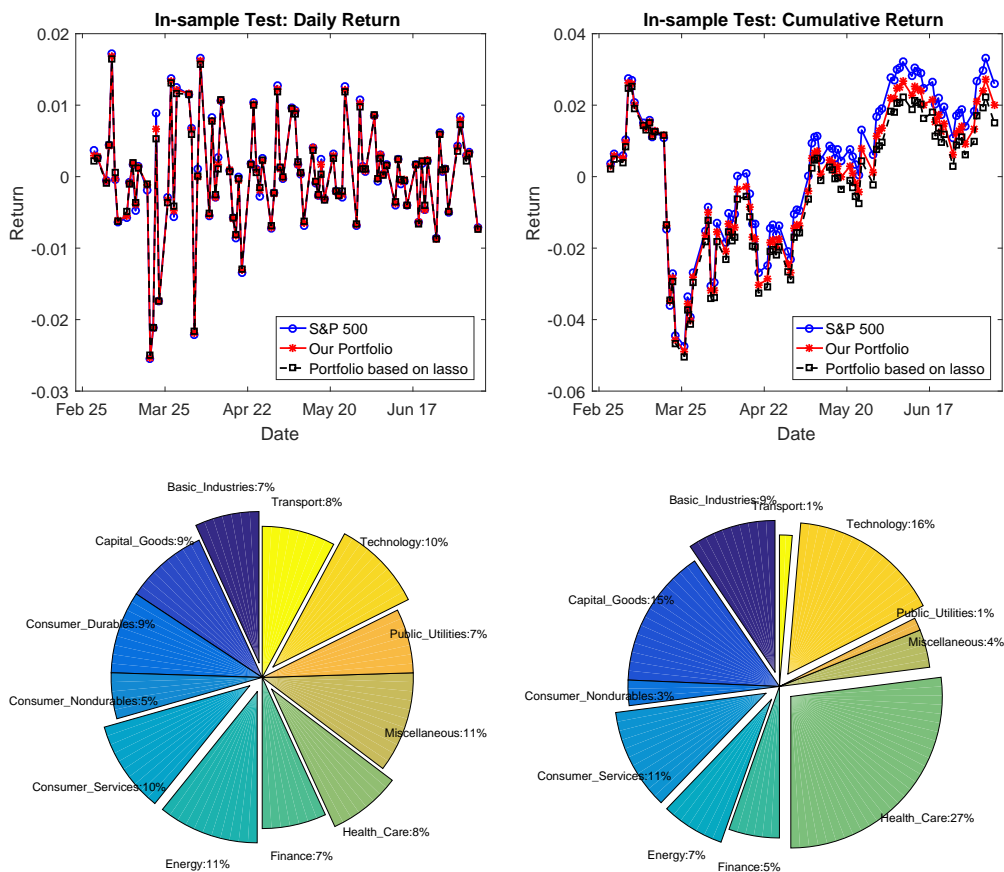


Figure 5: In-sample performance of two models for partial index tracking, and the percentage of selected stocks by sectors (left: exclusive lasso model, right: lasso model).

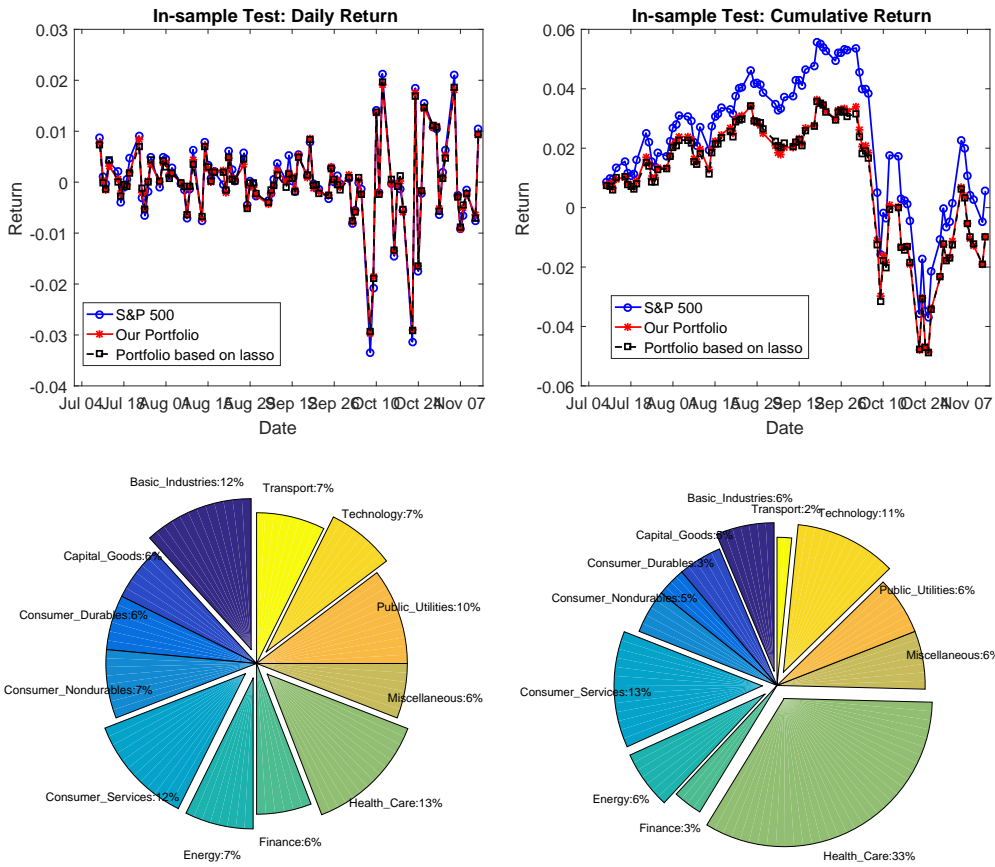


Figure 6: In-sample performance of two models for partial index tracking, and the percentage of selected stocks by sectors (left: exclusive lasso model, right: lasso model).